AIP | The Journal of Chemical Physics

Photoelectron spectroscopy of higher bromine and iodine oxide anions: Electron affinities and electronic structures of BrO2,3 and IO2–4 radicals

Hui Wen, Gao-Lei Hou, Wei Huang, Niranjan Govind, and Xue-Bin Wang

Citation: The Journal of Chemical Physics **135**, 184309 (2011); doi: 10.1063/1.3658858
View online: http://dx.doi.org/10.1063/1.3658858
View Table of Contents: http://scitation.aip.org/content/aip/journal/jcp/135/18?ver=pdfcov
Published by the AIP Publishing

Photoelectron spectroscopy of higher bromine and iodine oxide anions: Electron affinities and electronic structures of $BrO_{2,3}$ and IO_{2-4} radicals

Hui Wen,[1,2,a)] Gao-Lei Hou,[1,a),b)] Wei Huang,[2,c)] Niranjan Govind,[3,c)] and Xue-Bin Wang[1,4,c)]
[1]*Chemical & Materials Sciences Division, Pacific Northwest National Laboratory, P.O. Box 999, MS K8-88, Richland, Washington 99352, USA*
[2]*Laboratory of Environmental Spectroscopy, Anhui Institute of Optics & Fine Mechanics, Chinese Academy of Sciences, Hefei, Anhui 230031, China and Environmental Protection Key Laboratory of Optical Monitoring Technology, Ministry of Environmental Protection of China, China*
[3]*Environmental Molecular Sciences Laboratory, Pacific Northwest National Laboratory, P.O. Box 999, Richland, Washington 99352, USA*
[4]*Department of Physics, Washington State University, 2710 University Drive, Richland, Washington 99354, USA*

(Received 28 June 2011; accepted 19 October 2011; published online 14 November 2011)

This report details a photoelectron spectroscopy (PES) and theoretical investigation of electron affinities (EAs) and electronic structures of several atmospherically relevant higher bromine and iodine oxide molecules in the gas phase. PES spectra of BrO_2^- and IO_2^- were recorded at 12 K and four photon energies—355 nm/3.496 eV, 266 nm/4.661 eV, 193 nm/6.424 eV, and 157 nm/7.867 eV—while BrO_3^-, IO_3^-, and IO_4^- were only studied at 193 and 157 nm due to their expected high electron binding energies. Spectral features corresponding to transitions from the anionic ground state to the ground and excited states of the neutral are unraveled and resolved for each species. The EAs of these bromine and iodine oxides are experimentally determined for the first time (except for IO_2) to be 2.515 ± 0.010 (BrO_2), 2.575 ± 0.010 (IO_2), 4.60 ± 0.05 (BrO_3), 4.70 ± 0.05 (IO_3), and 6.05 ± 0.05 eV (IO_4). Three low-lying excited states along with their respective excitation energies are obtained for BrO_2 [1.69 (A $^2B_2$), 1.79 (B $^2A_1$), 1.99 eV (C $^2A_2$)], BrO_3 [0.7 (A $^2A_2$), 1.6 (B ^2E), 3.1 eV (C ^2E)], and IO_3 [0.60 (A $^2A_2$), 1.20 (B ^2E), ∼3.0 eV (C ^2E)], whereas six excited states of IO_2 are determined along with their respective excitation energies of 1.63 (A $^2B_2$), 1.73 (B $^2A_1$), 1.83 (C $^2A_2$), 4.23 (D $^2A_1$), 4.63 (E $^2B_2$), and 5.23 eV (F $^2B_1$). Periodate (IO_4^-) possesses a very high electron binding energy. Only one excited state feature with 0.95 eV excitation energy is shown in the 157 nm spectrum. Accompanying theoretical calculations reveal structural changes from the anions to the neutrals, and the calculated EAs are in good agreement with experimentally determined values. Franck-Condon factors simulations nicely reproduce the observed vibrational progressions for BrO_2 and IO_2. The low-lying excited state information is compared with theoretical calculations and discussed with their atmospheric implications. © *2011 American Institute of Physics*. [doi:10.1063/1.3658858]

I. INTRODUCTION

Since the landmark work by Rowland and Molina[1] demonstrating that chlorine monoxide and chlorine atoms are related to the catalytic reactions of ozone destruction in the stratosphere, there has been intense interest in characterizing halogen oxides and understanding their implications in atmospheric chemistry. In the last three decades, the majority of such research has been focused on chlorine oxides and related species, whose properties are now well studied.[2–11] Besides halogen atoms and monoxides, there is increasing evidence implying that higher halogen oxides and mixed oxides can actively participate in the overall ozone depletion cycles.[12,13] For example, chlorine dioxide (OClO) is involved in ozone depletion reactions via photodissociation to generate O + ClO and Cl + O_2 upon photoexcitation to the $^2A_2$ state.[6–11] Therefore, the detailed mechanism and dynamics of ClO_2 dissociation and its atmospheric implications have drawn much attention.[6–11] Beyond chlorine species, the importance of bromine oxides and related species in ozone depletion also has been established.[14–23] It has been suggested that bromine species is roughly 45 times more effective than chlorine for global ozone destruction.[18] Despite the important roles they play in the stratospheric chemistry, bromine oxides are relatively less studied compared with their chlorine counterparts, particularly for higher bromine oxides.[5,19–21] Experimental characterization of BrO_x is challenging, in part, due to their thermal meta-stability against decomposition ultimately into Br_2 and O_2.[21] Most of studies have been focused on BrO_2,[24–39]

a)Visiting student of alternate-sponsored fellowships (Pacific Northwest National Laboratory).
b)Permanent address: State Key Laboratory of Molecular Reaction Dynamics, Institute of Chemistry, Chinese Academy of Sciences, Beijing 100190, China.
c)Authors to whom correspondence should be addressed. Electronic addresses: xuebin.wang@pnnl.gov, huangwei@aiofm.ac.cn, and niri.govind@pnnl.gov.

with a only handful devoted to BrO_3.[21,40–47] Recently, there has been increasing interest in understanding the role of iodine chemistry in ozone depletion as well.[13,48–53] However, the knowledge about iodine oxides is even less robust than bromine species. Therefore, it is necessary to have a systematic spectroscopic approach to investigate intrinsic molecular properties of these bromine and iodine higher oxides. The obtained thermodynamic and spectroscopic information may assist in understanding their roles in the atmospheric chemistry.

Bromine dioxide has been relatively well studied. BrO_2 has been detected in the stratosphere as a possible nighttime bromine reservoir.[22,23] The first observation of gas-phase BrO_2 in the laboratory was reported by Butkovskaya *et al.*,[24] which suggested that paramagnetic BrO_2 molecules with lifetime >10 s among the products of the O + Br_2 reaction were found with the discharge flow-mass spectrometry technique. The first spectroscopic study (visible absorption) of gas phase BrO_2 was reported by Rattigan *et al.*[25] Since then, a numbers of studies have been devoted to investigate the properties of BrO_2 experimentally employing a variety of techniques,[23–29] including: rotational spectroscopy,[26] visible absorption in solid matrices,[27,28] photoionization,[19,29] and high-resolution ultraviolet/visable (UV/Vis) absorption spectroscopy.[30,31] The highly structured visible absorption spectrum of bromine dioxide radical, OBrO, observed in the 15 500–26 000 cm^{-1} region by Miller *et al.*,[31] was augmented by Franck-Condon simulations and high-level *ab initio* calculations, and concluded due to the dipole-allowed $C(^2A_2) \leftarrow X(^2B_1)$ electronic transition. Several theoretical investigations have been conducted to study the molecular structure, vibrational spectra, and energetics of BrO_2.[32–36] Inspired by well-resolved UV/Vis absorption spectra,[25,30,31] high-level *ab initio* calculations on the ground, as well as the low-lying excited states, have been reported.[31,37,38] Despite these impressive progresses, the low-lying excited states of $A(^2B_2)$ and $B(^2A_1)$ predicted to be in the proximity of $C(^2A_2)$ (Ref. 38) have not yet been probed experimentally due to extremely small dipole transitions from the ground $X(^2B_1)$ state. Being similar to ClO_2,[6,7] the photochemistry and photodissociation of BrO_2 and hence its atmospheric implications are expected to involve all three closed-lying states via spin-orbit and vibronic interactions following photoexcitation to $C(^2A_2)$.[39] Considering the significance of BrO_2 photodissociation in stratospheric ozone chemistry, it is highly desirable to experimentally study the low-lying excited states and compare them directly with the theoretical predictions.[31,38]

Despite the fact that its anion (BrO_3^-) is commonly found in solutions and solids,[40–44] understanding of the BrO_3 radical is particularly limited.[21] Except for the detection of the BrO_3 radical by photolysis of BrO_3^- aqueous solution[43] or radiation of solid crystals at cryogenic temperatures,[44] there is no other experimental report on this radical. A handful of theoretical studies have been performed to investigate the geometries, vibrational frequencies, heats of formation, and other properties of the most stable C_{3v} structure of bromine trioxide in the gas phase,[36,45] as well as low-lying excited states.[46] The electron affinities (EAs) of $BrO_{1–4}$ have been calculated.[47] To date, no gas phase spectroscopic study of BrO_3 has been reported.

Understanding the role of iodine chemistry in ozone depletion has attracted a lot of attention recently[13,48–53] and should provide a more complete view of halogen atmospheric chemistry. Iodine species undergo similar reactions in the troposphere due to the formation of its compounds in the marine boundary layer.[13,51–53] Iodine oxides have been known about for more than 100 years, but their properties remain poorly characterized. The detection of gas phase IO_2 was first reported in the thermal decomposition from I_2O_5,[54] and in halogen monoxide inter-reactions.[55] Gilles *et al.*[5] carried out a negative ion photoelectron spectroscopic study on OIO^- to probe the ground state of IO_2. The EA of OIO was determined to be 2.577 eV. The rotational spectrum of the OIO radical,[56] as well as visible absorption spectrum,[57] has been reported. Despite similar visible absorption and excitation transition,[57] IO_2 displays different photochemistry when compared to both ClO_2 and BrO_2. Upon the $C(^2A_2) \leftarrow X(^2B_1)$ excitation, the excited IO_2 exclusively dissociates to I + O_2 with the quantum yield close to one[51] with no IO + O being detected[58]—in contrast to both channels being observed for its lighter congeners.[6,38] Several theoretical calculations on thermodynamic properties of IO_2 have been reported.[13,52,59] The distinctly different dissociation mechanism of IO_2 and its atmospheric implications have stimulated a detailed, high-level *ab initio* computation study on the low-lying electronic states of OIO and their connection path to the dissociated products,[53] which predicted the $C(^2A_2)$ state of IO_2 is still more stable relative to IO + O product. Meanwhile, the I + O_2 channel involves an initial spin-orbit interaction between the $C(^2A_2)$ state and the nearby $B(^2A_1)$ followed by a strong vibronic interaction with the $A(^2B_2)$ state via an avoided crossing. An experimental probe on these three nearby electronic states will help to clarify the dissociation dynamics and verify theoretical predictions. In addition, there is no theoretical or experimental characterization for IO_3 and IO_4 reported.

In contrast to the neutral species, the halogen oxide anions are relatively stable (closed-shell) and commonly exist in condensed phases as an important class of anions in bulk materials. The transfer Gibbs energies for XO_3^- (X = Cl, Br, I) in water-methanol mixtures[60] and dissociation rate of HXO_3 (X = Cl, Br) in aqueous solution[41] have been reported. It has been suggested that these anions may also play a role in the upper stratospheric chemistry.[61] Their geometric structures and vibrational frequencies have been investigated using both vibrational spectroscopy[40,62] and theoretical calculations.[63,64]

Gas-phase anion photoelectron spectroscopy (PES) has been proven to be a powerful experimental technique, not only directly yielding adiabatic electron detachment energies (ADEs) of anions but also probing the ground and excited states of the corresponding neutral species.[65] By coupling with an electrospray ion source (ESI), many pristine anions in solutions can be readily transferred into the vacuum and probed by PES.[66] Unlike optical absorption spectroscopy, which is subject to stringent selection rules, PES often can access all electronic states within photon energy limits, including optically "dark" states of the neutral species. Lineberger and coworkers[5] performed the first PES study on XO^- (X = F, Cl, Br, I), $OClO^-$, and OIO^- at 351 nm and obtained the EAs and vibrational frequencies of the ground state

X ($^2B_1$) of ClO_2 and IO_2. Wang and Wang[2] conducted a PES investigation on ClO_x^- (x = 2–4) at various photon energies up to 7.8 eV. Along with the ground state, three low-lying electronic states, A($^2B_2$), B($^2A_1$), and C($^2A_2$) of ClO_2, and two electronic excited states, A($^2A_2$) and B(^2E) of ClO_3, were probed and compared with available theoretical predictions. This PES study on the A($^2B_2$) and B($^2A_1$) states of ClO_2, which are optically "dark" states but involved in photochemistry of ClO_2 species,[6,9] is significant and has stimulated a theoretical simulation on dissociation dynamics of ClO_2.[7]

In this paper, we present a systematic PES study of a series of higher halogen oxide anions: $BrO_{2,3}^-$ and IO_{2-4}^- using photon energies ranging from 3.496 eV (355 nm) to 7.867 eV (157 nm). The anions were readily generated from solutions using ESI. The high photon energy is essential for these species, which are expected to possess high electron binding energies for trioxides and above, and to interrogate the excited states of the corresponding neutrals. Besides the ground states, three low-lying excited states are obtained for BrO_2, BrO_3, and IO_3, with six excited states for IO_2 and one for IO_4. All spectra were taken at a temperature of 12 K, affording more accurate measurement of electron binding energies.[67,68] The obtained EAs of $BrO_{2,3}$ and $IO_{3,4}$ represent first experimental EA measurement for these important species. The unraveled excited state information provides valuable spectroscopic quantities to rationalize and foresee possible photochemistry of these atmospherically important molecules.

II. EXPERIMENTAL AND THEORETICAL DETAILS

A. Low-temperature photoelectron spectroscopy

The experiments were carried out with a low-temperature PES apparatus, which features an ESI source, a three-dimensional (3D) cryogenically controlled ion trap, a time-of-flight (TOF) mass spectrometer, and a magnetic-bottle electron analyzer.[69] It has been demonstrated that very cold ions can be created in the gas phase using cold traps.[70–74] To produce the desired anions, we used a 10^{-4} molar solution of the related salts $NaIO_3$, $NaIO_4$, and $NaBrO_3$ dissolved in a water/acetonitrile mixture solvent (1/3 volume ratio). IO_2^- and BrO_2^- were generated in the solutions via disproportionation reactions. The anions produced from ESI were guided by two radio frequency quadrupole ion guides followed by a 90° bender into a temperature-controlled Paul trap, where they were accumulated and collisionally cooled before being pulsed out into the extraction zone of a TOF mass spectrometer at a 10 Hz repetition rate. The ion trap was operated at 12 K in the current experiment.

For each PES experiment, the desired anions were first mass-selected and decelerated before being detached by a laser beam in the interaction zone of a magnetic bottle photoelectron analyzer. Four detachment photon energies were used in the current study: 193 nm (ArF, 6.424 eV) and 157 nm (F_2, 7.867 eV) from an excimer laser, and 266 nm (4.661 eV) and 355 nm (3.496 eV) from an Nd:YAG laser. All of the lasers were operated at a 20 Hz repetition rate with the ion beam off at alternating laser shots for shot-to-shot background subtraction. Photoelectrons were collected at nearly 100% efficiency by the magnetic bottle and analyzed in a 5.2 m long electron flight tube. TOF photoelectron spectra were collected and converted to kinetic energy spectra calibrated with the known spectra of I^- and $Cu(CN)_2^-$.[75] The electron binding energy spectra were obtained by subtracting the kinetic energy spectra from the detachment photon energies. The electron kinetic energy resolution was about 2%, i.e., 20 meV for 1 eV electrons.

B. Theoretical methods

Theoretical calculations were employed to study the geometries and electronic structures of halogen oxide anions and the corresponding neutral molecules. Geometrical optimizations were performed with density functional theory (DFT) using the hybrid B3LYP exchange-correlation functional[76] and the aug-cc-pvtz (for Br, O),[77] aug-cc-pvtz-pp (for I) basis set[78] obtained from the EMSL Basis Set Exchange (https://bse.pnl.gov/bse/portal). The ADE value of the anion is calculated as the energy difference between the anion and corresponding neutral radical at their respective optimized structures with zero-point energy corrections. All calculations were performed with the NWCHEM program.[79]

III. RESULTS

A. Photoelectron spectra

Figure 1 shows 12 K PES spectra of BrO_2^- at 355 (a), 266 (b), 193 (c), and 157 nm (d). A well-resolved, single vibrational progression was observed at 355 nm with the frequency of 785 ± 20 cm^{-1}. Due to effective vibrational cooling of ions at 12 K, no hot band transitions are expected. The ADE of BrO_2^-, or EA of BrO_2 radical, is determined from the first resolved transition (0–0) to be 2.515 ± 0.010 eV (Table I). At 266 nm, one extra band exhibits at high binding energy (4.1–4.6 eV) with a clear band gap from the ground state transition (X). The whole band at high binding energy is unraveled at 193 and 157 nm, spanning from 4.1 to 5.0 eV, which actually contains three partially resolved peaks, labeled A, B, and C (Figs. 1(c) and 1(d)). There is no other feature beyond 5.0 eV.

The PES spectra of IO_2^- at 12 K are shown in Fig. 2. Similar spectral patterns were observed at 355, 266, and 193 nm compared to BrO_2^-—a well vibrationally resolved ground state feature (X) at 355 nm and three partially resolved peaks (A, B, C) congested between 4.1 and 5.0 eV. The EA of 2.575 ± 0.010 eV for IO_2 measured from the 0–0 transition and 755 ± 20 cm^{-1} vibrational frequency are in excellent agreement with the previously reported values of 2.577 ± 0.008 eV and 765 ± 25 cm^{-1}.[5] At 157 nm, two more peaks (D and E) and a threshold for a possible third peak (F) are resolved in the 6.8–7.8 eV energy range.

The spectra of XO_3^- (X = Br and I) were measured only at 193 and 157 nm due to their expected high electron binding energy and are shown in Figs. 3 and 4, respectively. The 193 nm spectrum of BrO_3^- exhibits two peaks, X and A, with the peak positions at 4.85 and 5.5 eV and an onset of a third

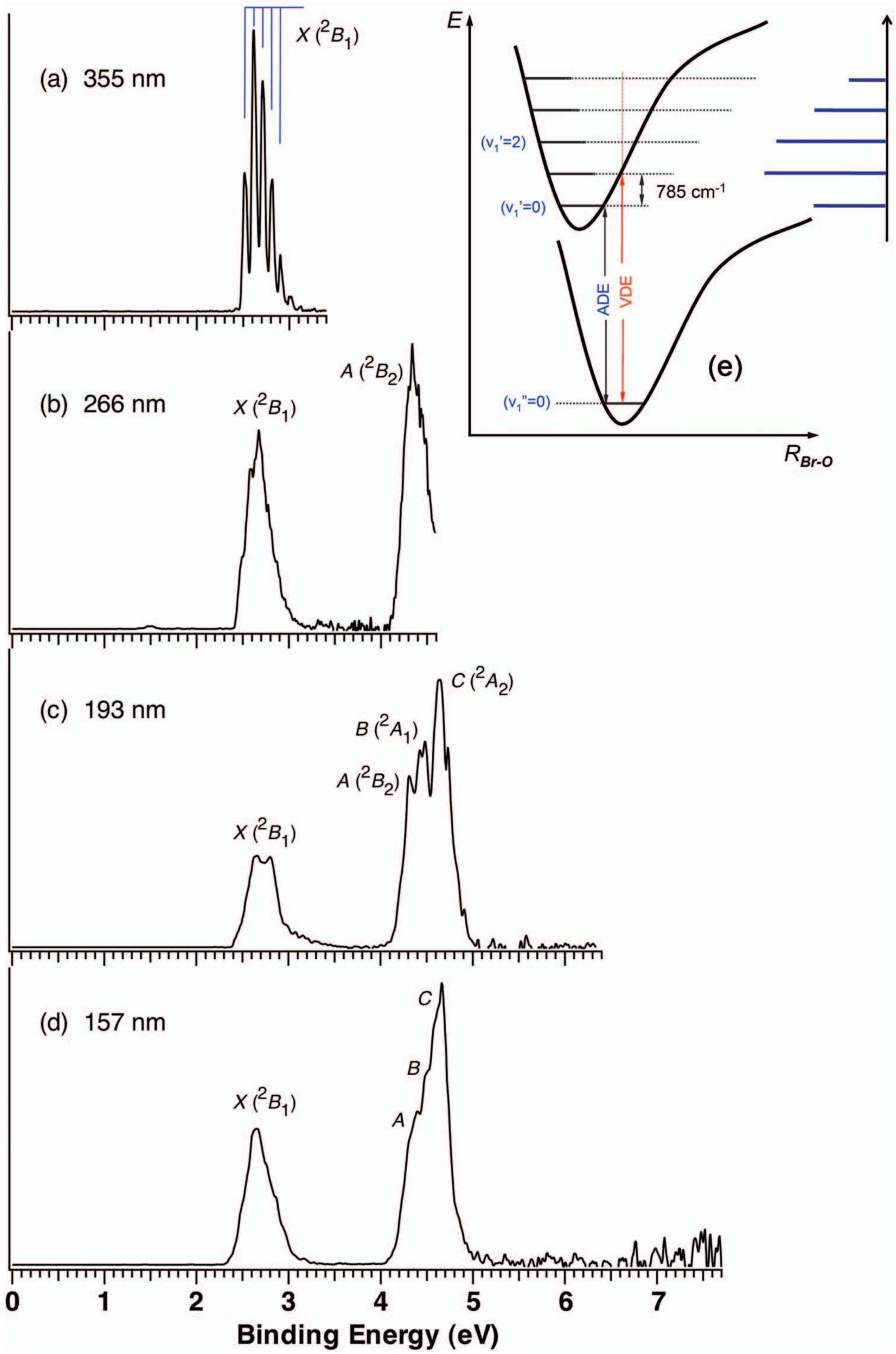

FIG. 1. Low-temperature (12 K) photoelectron spectra of BrO_2^- at (a) 355, (b) 266, (c) 193, and (d) 157 nm. The spectral assignment and vibrational progression are indicated. Schematic diagram for the transition from the ground state of the anion to the ground state of the neutral along the symmetric Br–O stretching coordinate and the simulated stick spectrum of Franck-Condon factors are shown in (e).

peak, B, at 6.3 eV, whereas the full band of B and the threshold of a fourth peak, C, are shown at 157 nm (Fig. 3). No vibrational structures were resolved in the spectra. The ADE was estimated by drawing a straight line at the leading edge of the ground state transition then adding a constant to the intercept with the binding energy axis to account for the instrumental resolution. The ADE of BrO_3^-, or EA of BrO_3, is estimated to be 4.60 ± 0.05 eV (Table II). The ADEs of the higher binding energy transitions were estimated in the same manner as the ground state feature X, while all vertical detachment energies (VDEs) were measured from the peak maximum of each band. The ADEs and VDEs of all observed features are listed in Table II. Similarly, three full bands (X, A, B) are seen at 193 nm, while an extra onset of a fourth band is revealed at 157 nm for IO_3^- (Fig. 4). The EA of IO_3, 4.70 ± 0.05 eV, is slightly higher than that of BrO_3, and all measured electron

TABLE I. Experimental and calculated adiabatic detachment energies (ADEs) and vertical detachment energies (VDEs) for BrO_2^- and IO_2^-; final state assignments for the ground- and low-lying-excited states of the corresponding neutral radicals; and calculated term value, T_e; and vertical excitation energy, ΔE from literatures (energy unit in eV).

		ADE			Excitation energy			
	Feature (state)	Expt.[a]	Calc.[b]	VDE[a]	ΔADE	ΔVDE	T_e	ΔE
BrO_2^-	X ($^2B_1$)	2.515 (0.01)	2.50	2.615 (0.01)	0	0	0	0
	Vib. Freq. (cm^{-1})	785 (20)	833					
	A ($^2B_2$)	4.20 (0.10)[c]		4.31 (0.05)	1.69	1.70	1.56[d]	2.43[e]
	B ($^2A_1$)	4.30 (0.10)[c]		4.45 (0.05)	1.79	1.84	2.03[d]	2.51[e]
	C ($^2A_2$)	4.50 (0.10)[c]		4.64 (0.05)	1.99	2.03	2.08[d] 1.97[d] (T_0)	2.69[e]
IO_2^-	X ($^2B_1$)	2.575 (0.01)	2.57	2.670 (0.01)	0	0	0	
	Vib. Freq. (cm^{-1})	755 (20)	787					
	A ($^2B_2$)	4.20 (0.10)[c]		4.32 (0.05)	1.63	1.65	1.54[f]	
	B ($^2A_1$)	4.30 (0.10)[c]		4.45 (0.10)[c]	1.73	1.78	1.96[f]	
	C ($^2A_2$)	4.40 (0.10)[c]		4.58 (0.10)[c]	1.83	1.91	2.07[f] (1.80)[g]	
	D ($^2A_1$)	6.80 (0.10)		6.96 (0.10)	4.23	4.29		
	E ($^2B_2$)	7.20 (0.10)		7.33 (0.10)	4.63	4.66		
	F ($^2B_1$)	~7.8		≥7.8 (0.1)	5.23	≥5.13		

[a]This work. Numbers in parentheses represent experimental error bars.
[b]This work. Calculated values are obtained at the B3LYP/aug-cc-pvtz (for Br, O) and aug-cc-pvtz-pp (for I) level of theory.
[c]Estimated with large uncertainty due to overlap of features.
[d]Experimental and theoretical term values from Ref. 31.
[e]Theoretical values from Ref. 38.
[f]Theoretical values from Ref. 53.
[g]Experimental values from Ref. 57.

binding energies of different peaks are listed in Table II. Overall, the spectral pattern of IO_3^- is similar to that of BrO_3^-, except there is an extra peak resolved at 5.0 eV within the X band probably caused by larger spin-orbit splitting effect. For IO_4^- (Fig. 5), there is one peak at 6.05 eV resolved at 193 nm, while an additional second peak at 7.0 eV exhibits at 157 nm. The ADE is found extremely high, which is consistent with the previous study on ClO_4^-.[2]

The obtained ADEs and VDEs for all observed spectral features are provided in Table I for BrO_2^- and IO_2^- (the ADEs for A, B, and C features were estimated with large uncertainty due to partial overlap of these features) while Table II lists features for BrO_3^-, IO_3^-, and IO_4^-. Tables I and II also list the ADE and VDE differences, ΔADEs and ΔVDEs, for the excited state transitions relative to the respective values of the ground states. ΔADEs can compare with the available term values, T_e of the corresponding excited states for the neutral molecules, while ΔVDEs resemble the vertical excitation energies of the neutrals at the anion's geometry. If the structural change from the anion's ground state to the ground state of the neutral is not substantial, the measured ΔVDEs can directly compare with the theoretically predicted vertical excitation energies, which were calculated at the neutral ground state geometry.

B. Theoretical results and Franck-Condon factors simulation

Electronic structure calculations were carried out to obtain the optimized geometries of the anions and neutrals, and to calculate ADEs in direct comparison with the experiments. For the dioxides and trioxides, both anions (closed-shell) and neutral radicals have the same symmetry, i.e., C_{2v} for XO_2^-/XO_2, and C_{3v} for XO_3^-/XO_3 (X = Br, I), respectively. The general geometric change following electron removal is that the X–O bond length is slightly shortened, and the X–O–X bond angle opened up (Fig. 6). While IO_4^- is a perfect tetrahedron molecule with T_d symmetry, the global minimum of the neutral IO_4 radical is found to adopt a C_{2v} structure (with the C_s structure almost degenerate) due to the expected Jahn-Teller effect. The calculated ADEs, listed in Table I and II, i.e., 2.50, 2.57, 4.48, 4.57, and 5.80 eV for BrO_2^-, IO_2^-, BrO_3^-, IO_3^-, and IO_4^-, respectively, are in good agreement with the experimental data. The calculated frequencies of the symmetric stretching mode for the BrO_2 and IO_2 neutral are in good accord with the observed values as well.

We have used the EZSPECTRUM, version 3.0 (Ref. 80) program to perform Franck-Condon factors (FCFs) calculations. The equilibrium geometries, harmonic frequencies, and normal mode vectors for BrO_2, BrO_2^-, IO_2, and IO_2^- are obtained from geometry optimization and ADE calculations described in the previous paragraph. For BrO_2, in order to get a good match between the calculated FCFs (Fig. 1(e)) and the experimental spectrum (Fig. 1(a)), we need to adjust the bond length of the BrO_2^- anion a little bit on the basis of the calculated bond length (from 1.733 Å to 1.726 Å) with the bond angle unchanged. For IO_2, the simulated FCFs based on the calculated geometries and frequencies for IO_2 and IO_2^- using calculations performed with NWCHEM are in excellent agreement with the observed spectrum without any adjustment (Fig. 2(e) vs. Fig. 2(a)).

IV. SPECTRAL ASSIGNMENT AND DISCUSSION

The PES spectral features in Figs. 1–5 represent transitions from the ground state of the anion (closed-shell) to

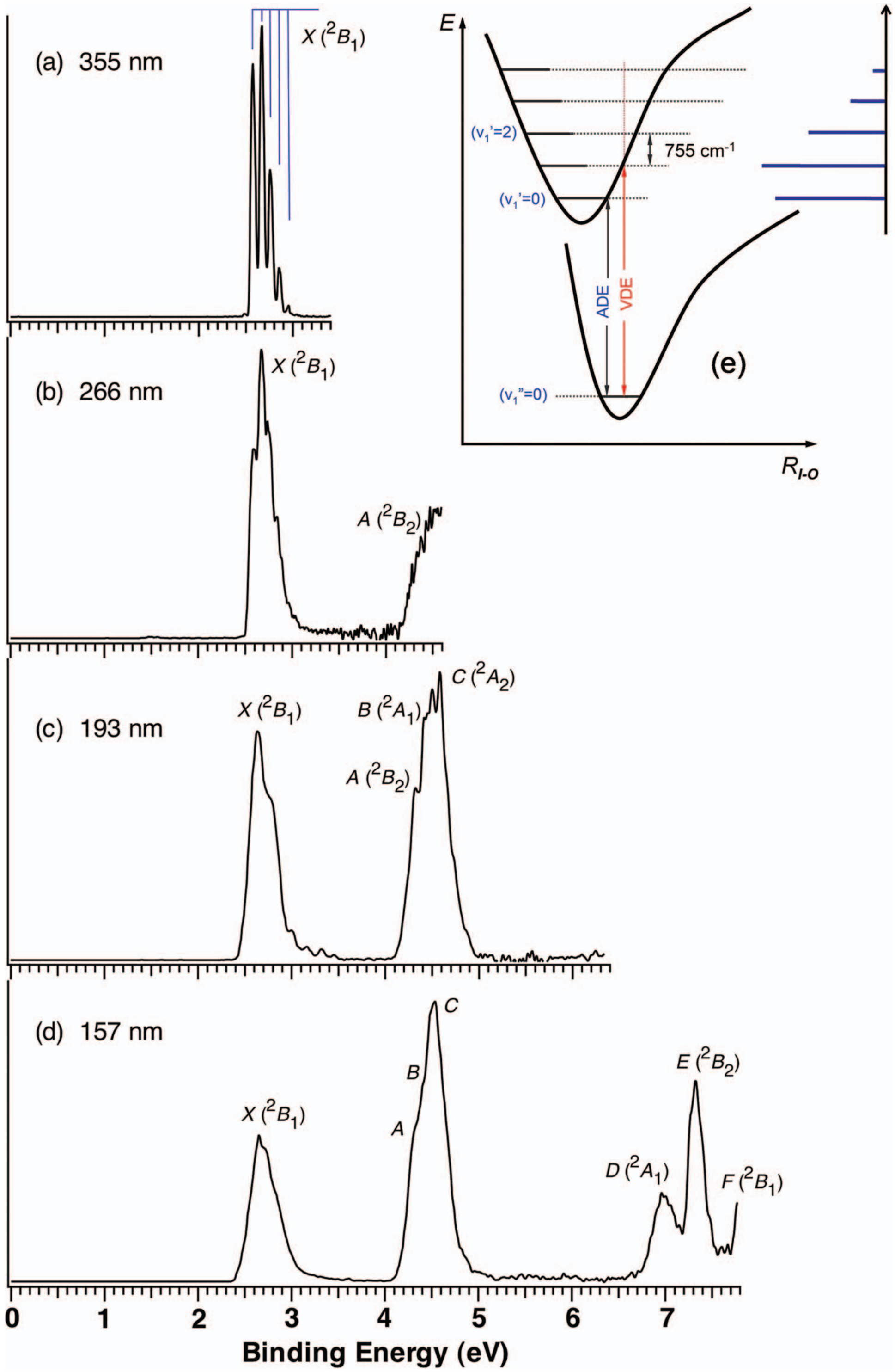

FIG. 2. Low-temperature (12 K) photoelectron spectra of IO_2^- at (a) 355, (b) 266, (c) 193, and (d) 157 nm. The spectral assignment and vibrational progression are indicated. Schematic diagram for the transition from the ground state of the anion to the ground state of the neutral along the symmetric I–O stretching coordinate and the simulated stick spectrum of Franck-Condon factors are shown in (e).

the ground and excited states of the corresponding neutral radical. In Koopmans' approximation, these features can be viewed alternatively as removing electrons from each occupied molecular orbitals (MOs) in the anion. Thus, the excited states of the neutral can be obtained from the ground state electronic configuration by single excitation to promote one electron from the deeper-occupied MOs to the upmost singly occupied MO. Although no excited state calculations are accompanied in this study, our spectral assignment was deduced based on the previous PES work of $ClO_{2\text{-}4}^-$,[2] confirmed by comparison with available theoretical predictions.

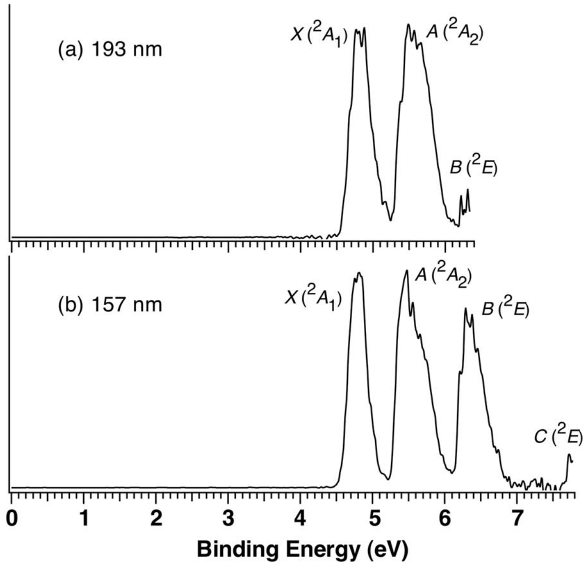

FIG. 3. Low-temperature (12 K) photoelectron spectra of BrO_3^- at (a) 193 and (b) 157 nm. The spectral assignment is indicated.

A. Halogen dioxide anions and neutrals: XO_2^- and $XO_2^\bullet$ (X = Br, I)

1. BrO_2^- and $BrO_2^\bullet$

All halogen dioxides have bent structures possessing C_{2v} symmetry. The 51 electrons of $BrO_2^\bullet$ are distributed among 26 MOs with the following configuration in the ground state: X $^2B_1$: core $(14a_1)^2(2b_2)^2(3a_2)^2(7b_1)^1$.[31] The microwave spectrum was analyzed to yield a bent molecule with Br–O bond length of 1.649 Å and O–Br–O bond angle of 114.44°.[81] The extra electron for the BrO_2^- anion is expected to reside on the singly occupied MO, $7b_1$, to form a closed-shell ground state ($^1A_1$). The BrO_2^- anion was previously predicted[63] to have a longer Br–O bond length, 1.758 Å, and a slightly smaller O–Br–O bond angle, 111.9° compared to $BrO_2^\bullet$. A similar structural change also was observed in the ClO_2^-.[2] Our calculations indicate the same trend of geometric changes upon electron detachment; i.e., 1.733 → 1.652 Å for Br–O bond length, and 112.2° → 113.8° for O–Br–O angle (Fig. 6). The reason for this structural change is due to the anti-bonding character of MO $7b_1$, where the extra electron is located. The 355 nm spectrum of BrO_2^- (Fig. 1(a)) appropriately reflects the geometric change during the transition of X $^2B_1$ ← X $^1A_1$ with the total symmetric stretching mode (υ_1) of the neutral dominant. The one dimensional FCF simulation (Fig. 1(e)) reproduces well the observed vibrationally resolved spectrum. The measured frequency of 785 ± 20 cm^{-1} compares excellently with that of 799.4 cm^{-1} obtained from the UV/Vis absorption spectrum,[31] as well as with the calculated value of 833 cm^{-1}.

Similar to ClO_2, three low-lying excited states, A($^2B_2$), B($^2A_1$), and C($^2A_2$), are predicted theoretically for BrO_2,[31] corresponding to single excitations from the $3a_2$, $2b_2$, and $14a_1$ orbitals into the singly occupied $7b_1$ orbital, respectively. The 193 and 157 nm spectra (Figs. 1(c) and 1(d)) clearly show that three partially resolved peaks, A, B, and C, reside within ∼1 eV range (4.1–5.1 eV). The measured excitation energies of these peaks relative to the ground state, ΔADEs, and ΔVDEs are given in Table I and are in qualitative agreement with the theoretically predicted term values and vertical excitation energies. In particular, the ΔADE of 1.99 eV for the C($^2A_2$) state accords excellently with the experimentally determined T_0 (1.97 eV).[31] Therefore, it is straightforward to assign the observed spectral features (shown in Fig. 1 and Table I). The EA of 2.515 ± 0.010 eV obtained in the current work is 0.15 eV higher than a previously predicted value of 2.36 eV,[47] but is in excellent agreement with our own calculated value of 2.50 eV.

Compared to the calculated geometry of BrO_2^- (1.733 Å; 112.2°), the bond length in each of these three excited states of the neutral remains almost the same (1.759, 1.775, and 1.785 Å) but with significant bond angle changes (85.6, 118.1, and 103.2°) for A, B, and C state, respectively.[31] Therefore, no symmetric stretching mode is expected for these transitions. Considering small frequencies of the bending mode and the near degeneracy of these three states, the three spectral features are expected to be congested and partially overlapped. The observed spectral pattern in Fig. 1 is consistent with the preceding expectation.

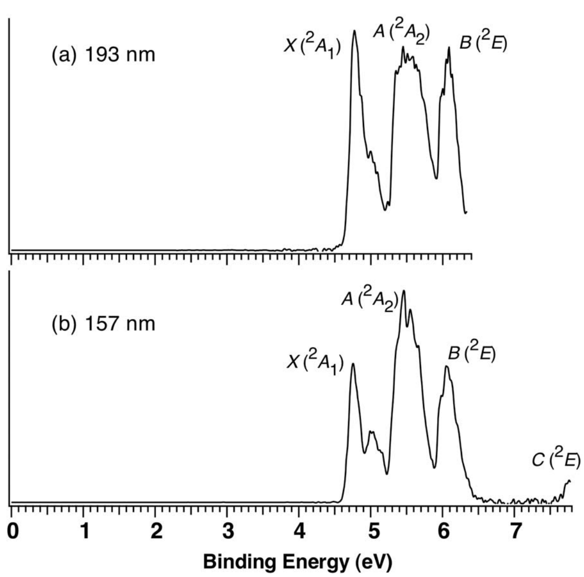

FIG. 4. Low-temperature (12 K) photoelectron spectra of IO_3^- at (a) 193 and (b) 157 nm. The spectral assignment is indicated.

2. IO_2^- and $IO_2^\bullet$

Iodine dioxide has been proposed to serve as the starting point for the formation of iodine aerosols in the marine boundary layer.[82,83] While IO_2 initially was believed to be remarkably stable with respect to the photodissociation channel of IO + O in the visible light,[58] it later was found to be facially dissociated into I + O_2 (Ref. 51) via spin-orbit and vibronic interactions involving three low-lying excited states[53] similar to those in BrO_2 and ClO_2. A previous absorption spectrum indicated a term value of 1.80 eV for the C($^2A_2$) state,[57] and a recent *ab initio* calculation predicted term values

TABLE II. Experimental and calculated adiabatic detachment energies (ADEs) and vertical detachment energies (VDEs) for BrO_3^- and $IO_{3\text{-}4}^-$; final state assignments for the ground- and low-lying-excited states of the corresponding neutral radicals; and calculated vertical excitation energy, ΔE from literatures (energy unit in eV).

	Feature (state)	ADE[c] Expt.[a]	ADE[c] Calc.[b]	VDE[a]	Excitation energy ΔADE	Excitation energy ΔVDE	Excitation energy ΔE[c]
BrO_3^-	X ($^2A_1$)	4.60 (0.05)	4.48	4.85 (0.10)	0	0	0
	A ($^2A_2$)	5.30 (0.10)		5.50 (0.10)	0.7	0.65	0.72
	B (^2E)	6.20 (0.10)		6.30 (0.10)	1.6	1.45	1.50
	C (^2E)	∼7.7		∼7.7	3.1	≥2.85	2.37
IO_3^-	X ($^2A_1$)	4.70 (0.05)	4.57	4.77 (0.05)	0	0	
	A ($^2A_2$)	5.30 (0.10)		5.45 (0.10)	0.60	0.68	
	B (^2E)	5.90 (0.10)		6.05 (0.10)	1.20	1.28	
	C (^2E)	∼7.7		∼7.8	∼3.0	∼3.0	
IO_4^-	X ($^2B_1$)	6.05 (0.05)	5.80	6.30 (0.10)	0	0	
	A ($^2B_2$)	7.00 (0.05)		7.00 (0.05)	0.95	0.7	

[a]This work. Numbers in parentheses represent experimental error bars.
[b]This work. Calculated values are obtained at the B3LYP/aug-cc-pvtz (for Br, O) and aug-cc-pvtz-pp (for I) level of theory.
[c]Theoretical values from Ref. 46.

of 1.54, 1.96, and 2.07 eV for A($^2B_2$), B($^2A_1$), and C($^2A_2$), respectively.[53]

The first feature X (2.5–3.0 eV) in the PES spectra of IO_2 (Fig. 2) corresponds to the transition from the ground state of the anion ($^1A_1$) to the ground state of the neutral ($^2B_1$). Upon removal of the extra electron, there are sizable structural changes (bond length: 1.860 → 1.802 Å; bond angle: 108.3° → 110.0° from Ref. 53; and 1.889 → 1.825 Å and 109.7°→ 110.5° from our calculations). The profile of feature X is dominant with the single vibrational progression of the total symmetric stretching mode in the neutral ground state, and is well reproduced from the FCFs simulation (Fig. 2(a) vs. Fig. 2(e)). The frequency obtained from the 355 nm spectrum (Fig. 2(a)) is 755 ± 20 cm^{-1}, consistent with an earlier reported value[5] of 765 ± 20 cm^{-1}, and with the calculated one of 787 cm^{-1}.The EA of IO_2, measured from the first resolved peak in the 355 nm spectrum, is 2.575 ± 0.010 eV, which also indicates excellent agreement with a previously reported value (2.577 ± 0.008 eV),[5] and the current calculated value of 2.57 eV.

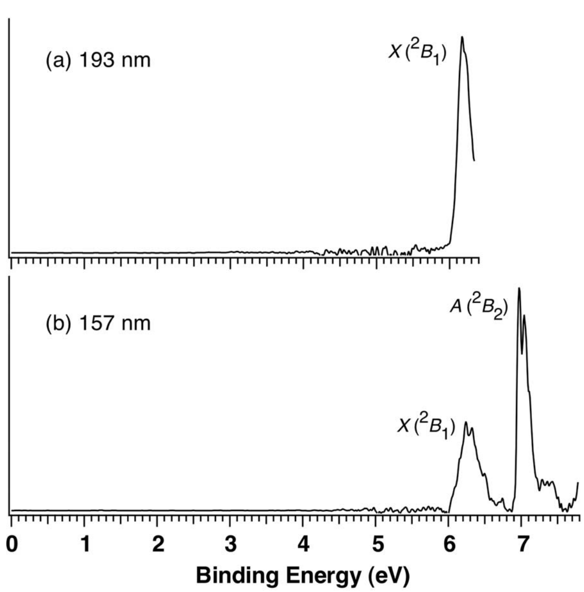

FIG. 5. Low-temperature (12 K) photoelectron spectra of IO_4^- at (a) 193 and (b) 157 nm. The spectral assignment is indicated.

Three features are discernibly resolved for the spectral band between 4.1 and 5.0 eV at 193 and 157 nm (Figs. 2(c) and 2(d)), most likely corresponding to transitions to the three predicted low-lying excited states, A($^2B_2$), B($^2A_1$), and C($^2A_2$). The estimated excitation energies (ΔADEs and ΔVDEs) for these three peaks qualitatively agree with the theoretical term values,[53] and the assigned ΔADE for C($^2A_2$) is in excellent accord with the term value determined from a previous absorption study[57] (Table I). All these further support the described assignment.

Three more spectral features, D, E, and F, are revealed at a very high binding energy range: 6.8–7.8 eV at 157 nm. No similar states were observed for BrO_2^- or for ClO_2^- at 157 nm.[2] They represent a set of excited states beyond the first three for IO_2. No previous study has been reported for these states. Herein, we make the tentative assignment for these states, D($^2A_1$), E($^2B_2$), and F($^2B_1$), according to the energy level scheme for ionization of ClO_2.[84] Their energetic information is shown in Table I.

B. Halogen trioxides anion and corresponding neutral molecules: XO_3^- and $XO_3^\bullet$ (X = Br, I)

Halogen trioxide anions are common anionic species in solution and solid with pyramidal equilibrium structures (C_{3v} symmetry) and $^1A_1$ ground state.[2,45–47] The electron configuration of BrO_3^- for the ground state[47] is: $(8e)^4(9e)^4(1a_2)^2(11a_1)^2$, which is similar to ClO_3^-.[2] Therefore, the three spectral features and a fourth onset shown in 157 nm spectrum (Fig. 3) are assigned accordingly by detaching one electron from the respective frontier occupied MOs, i.e., X($^2A_1$), A($^2A_2$), B(^2E), and C(^2E). The EA of BrO_3, measured from the rising edge of the X peak, is 4.60 ± 0.05 eV, in a reasonable agreement with the calculated value of 4.48 eV, but appreciably lager than the previously predicted EA value of 4.32 eV.[47] The electron binding

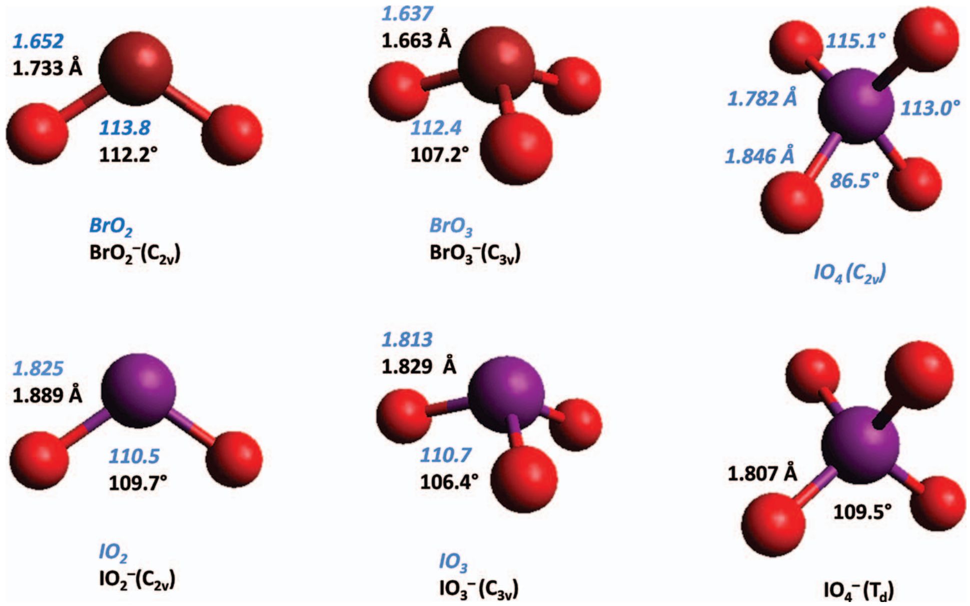

FIG. 6. Optimized structures of halogen oxide anions (normal typeface) and neutrals (italic typeface) at the B3LYP/aug-cc-pvtz (for Br, O); aug-cc-pvtz-pp (for I) level of theory. Molecular symmetry, bond length (in Å), and bond angle are indicated.

energies of all observed peaks are listed in Table II. The measured excitation energies for the excited states (ΔADEs and ΔVDEs) are in good agreement with a recent theoretical calculation[46] (Table II), supporting our spectral assignment. Upon removal of the extra electron, i.e., $BrO_3^- \rightarrow BrO_3^\bullet$, Br–O bond length shortens slightly, while the bond angle increases (Fig. 6) in the same trend observed for the halogen dioxides. The moderate spectral widths observed in the spectra are also consistent with the predicted bond length and angle changes.

To date, there has been no theoretical or experimental characterization reported for the isolated IO_3 radical. Therefore, we make a similar assignment for the electronic states of IO_3 based on the similarity of the spectral pattern between IO_3^- and BrO_3^-. The ADE of IO_3^-, or EA of IO_3, is determined to be 4.70 ± 0.05 eV, and compared reasonably to the calculated EA value of 4.57 eV. Similar structural changes as BrO_3^-/BrO_3 are observed from IO_3^- to IO_3 (Fig. 6). The obtained excited state energetic information about IO_3 represents the first characterization for these states and provides valuable experimental data to benchmark future theoretical calculations.

C. Periodate anion and the corresponding neutral: IO_4^- and $IO_4^\bullet$

Periodate is the conjugate base of periodic acid and predominate in neutral or weak acid conditions. Like its lighter elements congeners,[2,47,63] IO_4^- has a tetrahedral T_d structure. The iodine element has a formal +7 oxidation state with all *p* electrons being paired with the four oxygen atoms. Thus, the extra electron is shared equally by the four oxygen atoms, resulting in an extremely high binding energy. It also is expected that the IO_4 radical neutral (open shell) cannot maintain a T_d structure due to Jahn-Teller effect. Our calculations indicate a C_{2v} structure for IO_4 with a C_s one almost degenerate (Fig. 6), consistent with the results for both ClO_4 and BrO_4 (C_{2v} symmetry).[2,47,85,86] As such, the two spectral features observed at 157 nm are assigned due to $X(^2B_1)$ and $A(^2B_2)$ states of IO_4 (Fig. 5). Their electron binding energies are provided in Table II. The EA of IO_4 is quite high, 6.05 ± 0.05 eV from the experimental measurement and 5.80 eV from the calculations, even higher than the theoretically predicted EA of BrO_4 (5.28 eV) (Ref. 47) and the experimentally measured EA of ClO_4 (5.25 eV).[2]

D. Electron affinities of halogen oxides

The EAs of halogen dioxides are found to increase with halogen size, from 2.140 eV (ClO_2) (Ref. 5) to 2.515 eV (BrO_2) and to 2.575 eV (IO_2). Similar trends exist in the halogen monoxides.[5] The observation of apparently increasing electron stabilization in heavy halogen species probably is related to the longer bond length for heavy elements, resulting in a more delocalized charge density. The EAs of XO_3 are found to follow the same trend: EA of ClO_3 (4.25 eV)[2] < EA of BrO_3 (4.60 eV) < EA of IO_3 (4.70 eV). Although the PES spectra of BrO_4^- is not reported here, it is expected that EA (IO_4) > EA (BrO_4) > EA (ClO_4). This would bracket the electron affinity of BrO_4 between 5.25 and 6.05 eV in accord with the recently predicted EA of 5.28 eV.[47]

V. CONCLUSIONS

We report herein a systematic PES study on bromine and iodine oxide anions at several fixed photon energies up to 7.867 eV. The high photon energy used is essential for obtaining the EAs and electronic excited state information. Except for IO_2, the EAs of other neutral halogen oxides are experimentally determined for the first time to be 2.515

± 0.010 (BrO_2), 2.575 ± 0.010 (IO_2), 4.60 ± 0.05 (BrO_3), 4.70 ± 0.05 (IO_3), and 6.05 ± 0.05 eV (IO_4).

Taking advantage of the ubiquity of those anions in solutions, we have demonstrated that the ESI-PES approach is an ideal experimental technique to directly measure EAs and investigate electronic structures of the halogen oxides neutral radicals in the gas phase, particularly considering some of the radicals are not even thermodynamically stable. In addition, PES can access optically "dark" states complementary to the absorption spectroscopy. This is significant because the low-lying "dark" states, such as A($^2B_2$), and B($^2A_1$) in the halogen dioxides, are directly involved in the photochemistry and photodissociation processes of these species in the stratosphere. To date, our knowledge about these states is based largely on theoretical predictions.[6,37,38,46,53] The current work represents the first experimental (spectroscopic) probe aimed at providing direct energetic information to characterize these excited states in comparison with available theoretical predictions and to benchmark future theoretical studies.

ACKNOWLEDGMENTS

This work was supported by the Division of Chemical Sciences, Geosciences, and Biosciences, Office of Basic Energy Sciences, U.S. Department of Energy (DOE), and was performed using the Environmental Molecular Sciences Laboratory (EMSL), a national scientific user facility sponsored by DOE's Office of Biological and Environmental Research and located at Pacific Northwest National Laboratory (PNNL). PNNL is operated by Battelle for the DOE under Contract No. DE-AC05-76RL01830. W.H. wishes to thank the National Natural Science Foundation of China (Grant No. 21073196) for financial support. The FCF simulation was conducted using the resources of the iOpenShell Center for Computational Studies of Electronic Structure and Spectroscopy of Open-Shell and Electronically Excited Species (http://iopenshell.usc.edu) supported by the National Science Foundation through the CRIF:CRF program.

[1] M. J. Molina and F. S. Rowland, Nature (London) **249**, 810 (1974).
[2] X. B. Wang and L. S. Wang, J. Chem. Phys. **113**, 10928 (2000).
[3] M. M. Meyer and S. R. Kass, J. Phys. Chem. A **114**, 4086 (2010).
[4] J. S. Francisco and S. P. Sander, J. Chem. Phys. **99**, 2897 (1993).
[5] M. K. Gilles, M. L. Polak, and W. C. Lineberger, J. Chem. Phys. **96**, 8012 (1992).
[6] Q. Meng and M. B. Huang, J. Phys. Chem. A **115**, 2692 (2011).
[7] G. M. Krishnan and S. Mahapatra, J. Chem. Phys. **118**, 8715 (2003).
[8] H. F. Davis and Y. T. Lee, J. Chem. Phys. **105**, 8142 (1996).
[9] K. A. Peterson and H. J. Werner, J. Chem. Phys. **105**, 9823 (1996).
[10] K. A. Peterson and H. J. Werner, J. Chem. Phys. **96**, 8948 (1992).
[11] K. A. Peterson, J. Chem. Phys. **109**, 8864 (1998).
[12] M. Von Hobe, Science **318**, 1878 (2007).
[13] D. J. Grant, E. B. Garner III, M. H. Matus, M. T. Nguyen, K. A. Peterson, J. S. Francisco, and D. A. Dixon, J. Phys. Chem. A **114**, 4254 (2010).
[14] L. A. Barrie, J. W. Bottenheim, R. C. Schnell, P. J. Crutzen, and R. A. Rasmussen, Nature (London) **334**, 138 (1988).
[15] G. L. Bras and U. Platt, Geophys. Res. Lett. **22**, 599, doi:10.1029/94GL03334 (1995).
[16] R. P. Wayne, G. Poulet, P. Biggs, J. P. Burrows, R. A. Cox, P. J. Crutzen, G. D. Hayman, M. E. Jenkin, G. L. Bras, G. K. Moortgat, U. Platt, and R. N. Schindler, Atmos. Environ. **29**, 2677 (1995).
[17] K. Yagi, J. Williams, N. Y. Wang, and R. J. Cicerone, Science **267**, 1979 (1995).
[18] J. S. Daniel, S, Solomon, R. W. Portmann, and R. R. Garcia, J. Geophys. Res. **104**, 23871, doi:10.1029/1999JD900381 (1999).
[19] R. B. Klemm, R. P. Thorn, Jr., L. J. Stief, T. J. Buckley, and R. D. Johnson III, J. Phys. Chem. A **105**, 1638 (2001).
[20] M. W. Chase, J. Phys. Chem. Ref. Data **25**, 1069 (1996).
[21] K. Seppelt, Acc. Chem. Res. **30**, 111 (1997).
[22] J. B. Renard, M. Pirre, and C. Robert, J. Geophys. Res. **103**, 25383, doi:10.1029/98JD01805 (1998).
[23] M. P. Chipperfield, T. Glassup, I. Pundt, and O. V. Rattigan, Geophys. Res. Lett. **25**, 3575, doi:10.1029/98GL02759 (1998).
[24] N. I. Butkovskaya, I. I. Morozov, V. L. Talrose, and E. S. Vasiliev, Chem. Phys. **79**, 21 (1983).
[25] O. V. Rattigan, R. L. Jones, and R. A. Cox, Chem. Phys. Lett. **230**, 121 (1994).
[26] H. S. P. Müller, C. E. Miller, and E. A. Cohen, J. Chem. Phys. **107**, 8292 (1997).
[27] J. Kölm, A. Engdahl, O. Schrems, and B. Nelander, Chem. Phys. **214**, 313 (1997).
[28] Y. C. Lee and Y. P. Lee, J. Phys. Chem. A **104**, 6951 (2000).
[29] R. P. Thorn, Jr., L. J. Stief, T. J. Buckley, R. D. Johnson III, P. S. Monks, and R. B. Klemm, J. Phys. Chem. A **103**, 8384 (1999).
[30] G. Knight, A. R. Ravishankara, and J. B. Burkholder, J. Phys. Chem. A **104**, 11121 (2000).
[31] C. E. Miller, S. L. Nickolaisen, J. S. Francisco, and S. P. Sander, J. Chem. Phys. **107**, 2300 (1997).
[32] L. F. Pacios and P. C. Gómez, J. Phys. Chem. A **101**, 1767 (1997).
[33] J. S. Francisco, Chem. Phys. Lett. **288**, 307 (1998).
[34] M. Alcami, O. Mó, M. Yáñez, and I. L. Cooper, J. Chem. Phys. **112**, 6131 (2000).
[35] M. Alcami and I. L. Cooper, J. Chem. Phys. **108**, 9414 (1998).
[36] M. A. Workman and J. S. Francisco, Chem. Phys. Lett. **293**, 65 (1998).
[37] K. A. Peterson, J. Chem. Phys. **109**, 8864 (1998).
[38] R. Vetter, T. Ritschel, L. Zülicke, and K. A. Peterson, J. Phys. Chem. A **107**, 1405 (2003).
[39] K. J. Yuan, Z. Sun, S. L. Cong, and N. Lou, J. Chem. Phys. **123**, 064316 (2005).
[40] H. H. Eysel, K. G. Lipponer, C. Oberle, and I. Zahn, Spectrochim. Acta, Part A. Molecular and Biomolecular Spectroscopy **48**, 219 (1992).
[41] W. A. Alves, C. A. Téllez, S. O. Sala, P. S. Santos, and R. B. Faria, J. Raman Spectrosc. **32**, 1032 (2001).
[42] D. J. Gardiner, R. B. Girling, and R. E. Hester, J. Mol. Struct. **13**, 105 (1972).
[43] Z. Zuo and Y. Katsumura, J. Chem. Soc. Faraday Trans. **94**, 3577 (1998).
[44] J. R. Byberg, J. Chem. Phys. **83**, 919 (1985).
[45] L. F. Pacios and P. C. Gómez, Chem. Phys. Lett. **289**, 412 (1998).
[46] Y. Li and J. S. Francisco, J. Chem. Phys. **112**, 8866 (2000).
[47] Y. Xie, H. F. Schaefer III, Y. Wang, X. Y. Fu, and R. Z. Liu, Molec. Phys. **98**, 879 (2000).
[48] W. L. Chameides and D. D. Davis, J. Geophys. Res. **85**, 7383, doi:10.1029/JC085iC12p07383 (1980).
[49] S. Solomon, R. R. Garcia, and A. R. Ravishankara, J. Geophys. Res. **99**, 20491, doi:10.1029/94JD02028 (1994).
[50] S. Solomon, J. B. Burkholder, A. R. Ravishankara, and R. R. Garcia, J. Geophys. Res. **99**, 20929, doi:10.1029/94JD01833 (1994).
[51] J. C. G. Martin, S. H. Ashworth, A. S. Mahajan, and J. M. C. Plane, Geophys. Res. Lett. **36**, L09802, doi:10.1029/2009GL037642 (2009).
[52] N. Kaltsoyannis and J. M. C. Plane, Phys. Chem. Chem. Phys. **10**, 1723 (2008).
[53] K. A. Peterson, Mol. Phys. **108**, 393 (2010).
[54] M. H. Studier and J. L. Huston, J. Phys. Chem. **71**, 457 (1967).
[55] D. M. Rowley, W. J. Bloss, R. A. Cox, and R. L. Jones, J. Phys. Chem. A **105**, 7855 (2001).
[56] C. E. Miller and E. A. Cohen, J. Chem. Phys. **118**, 1 (2003).
[57] S. Himmelmann, J. Orphal, H. Bovensmann, A. Richter, A. Ladstätter-Weissenmayer, and J. P. Burrows, Chem. Phys. Lett. **251**, 330 (1996).
[58] T. Ingham, M. Cameron, and J. N. Crowley, J. Phys. Chem. A **104**, 8001 (2000).
[59] A. Misra and P. Marshall, J. Phys. Chem. A **102**, 9056 (1998).
[60] J. Benko, O. Vollárová, I. Černušák, and A. Pappová, J. Chem. Soc. Faraday Trans. **92**, 4935 (1996).
[61] S. S. Prasad, Ann. Geophys. **13**, 296 (1995).
[62] D. J. Gardiner, R. B. Girling, and R. E. Hester, J. Mol. Struct. **13**, 105 (1972).
[63] C. Oberle and H. H. Eysel, J. Mol. Struct.: THEOCHEM **280**, 107 (1993).

[64]B. D. El-Issa and A. Hinchliffe, J. Mol. Struct. **67**, 317 (1980).
[65]J. C. Rienstra-Kiracofe, G. S. Tschumper, H. F. Schaefer III, S. Nandi, and G. B. Ellison, Chem. Rev. **102**, 231 (2002).
[66]X. B. Wang and L. S. Wang, Annu. Rev. Phys. Chem. **60**, 105 (2009).
[67]X. B. Wang, Q. Fu, and J. L. Yang, J. Phys. Chem. A **114**, 9083 (2010).
[68]X. B. Wang and S. S. Xantheas, J. Phys. Chem. Lett. **2**, 1204 (2011).
[69]X. B. Wang and L. S. Wang, Rev. Sci. Instrum. **79**, 073108 (2008).
[70]D. Gerlich, Adv. Chem. Phys. **82**, 1 (1992).
[71]O. V. Boyarkin, S. R. Mercier, A. Kamariotis, and T. R. Rizzo, J. Am. Chem. Soc. **128**, 2816 (2006).
[72]J. Zhou, G. Santambrogio, M. Brummer, D. T. Moore, L. Woste, G. Meijer, D. M. Neumark, and K. R. Asmis, J. Chem. Phys. **125**, 111102 (2006).
[73]X. B. Wang, X. P. Xing, and L. S. Wang, J. Phys. Chem. A **112**, 13271 (2008).
[74]M. Z. Kamrath, R. A. Relph, T. L. Guasco, C. M. Leavitt, and M. A. Johnson, Int. J. Mass Spectrom. **300**, 91 (2011).
[75]X. B. Wang, Y. L. Wang, J. Yang, X. P. Xing, J. Li, and L. S. Wang, J. Am. Chem. Soc. **131**, 16368 (2009).
[76]P. J. Stephens, F. J. Devlin, C. F. Chabalowski, and M. J. Frisch, J. Phys. Chem. **98**, 11623 (1994).
[77]T. H. Dunning, Jr., J. Chem. Phys. **90**, 1007 (1989); A. K. Wilson, D. E. Woon, K. A. Peterson, and T. H. Dunning, Jr., J. Chem. Phys. **110**, 7667 (1999).
[78]K. A. Peterson, B. C. Shepler, D. Figgen, and H. Stoll, J. Phy. Chem. A **110**, 13877 (2006).
[79]M. Valiev, E. J. Bylaska, N. Govind, K. Kowalski, T. P. Straatsma, H. J. J. van Dam, D. Wang, J. Nieplocha, E. Apra, T. L. Windus, and W. A. de Jong, Comput. Phys. Commun. **181**, 1477 (2010).
[80]V. A. Mozhayskiy and A. I. Krylov, EZSPECTRUM, version 3.0, see http://iopenshell.usc.edu/downloads.
[81]H. S. P. Müller, C. E. Miller, and E. A. Cohen, Angew. Chem. Int. Ed. **35**, 2129 (1996).
[82]B. J. Allan, J. M. C. Plane, and G. McFiggans, Geophys. Res. Lett. **28**, 1945, doi:10.1029/2000GL012468 (2001).
[83]T. Hoffmann, T. C. D. O'Dowd, and J. H. Seinfeld, Geophys. Res. Lett. **28**, 1949, doi:10.1029/2000GL012399 (2001).
[84]R. Flesch, E. Rühl, K. Hottmann, and H. Baumgärtel, J. Phys. Chem. **97**, 837 (1993).
[85]T. J. Van Huis and H. F. Schaefer III, J. Chem. Phys. **106**, 4028 (1997).
[86]A. Beltrán, J. Andrés, S. Noury, and B. Silvi, J. Phys. Chem. A **103**, 3078 (1999).